

# **Response to reviewers for the paper “Aging impact on sources, volatility, and viscosity of organic aerosols in the Chinese outflows”**

**By Tingting Feng et al.**

We appreciate the reviewers' comments and support for the publication of this manuscript. Following the reviewer's suggestions, we have carefully revised the manuscript. To facilitate the review process, we have copied the reviewers' comments in black text. Our responses are in blue font. We have responded to all the referee comments and made alterations to our paper (**in bold text**).

## **Anonymous Referee #1**

Quantifications of the physicochemical properties, particularly volatility and viscosity, of OA are vital to understanding its environmental and climate effects. Feng et al. deployed HR-AMS coupled with a TD to investigate the aging impact on sources, volatility, and viscosity of OA in a regional receptor site of metropolitan emissions in North China Plain. They find that the volatility of OA in this receptor site is generally lower than those in previous field studies, indicating the large impact of atmospheric aging on the OA oxidation levels during transport. As well, the phase state of ambient OA is investigated from the estimated viscosity. The results have important implications for the understanding of the aging impact on OA volatility and viscosity. The methods are solid and the manuscript is well written. It can be recommended for publication after addressing the following minor comments.

### **Specific comments:**

**R1.1:** Section 2.2.1 HR-ToF-AMS: Which mode is the AMS running at? Only V mode? What's the time resolution?

**A1.1:** We only used V mode in this campaign, with the time resolution of 1 minute for ambient sampling and 2.5 minutes for TD sampling. To clarify this, we updated the sampling mode in Fig. S1 and modified

the original sentences as:

“All the AMS quantification and elemental ratio data used here were based on the “V” mode at a time resolution of 1 minute for the ambient dataset and 2.5 minutes for TD sampling (Fig. S1). The AMS data were analyzed with the software of Squirrel (v1.62G) and PIKA (V. 1.22G) based on Igor pro 6.37”

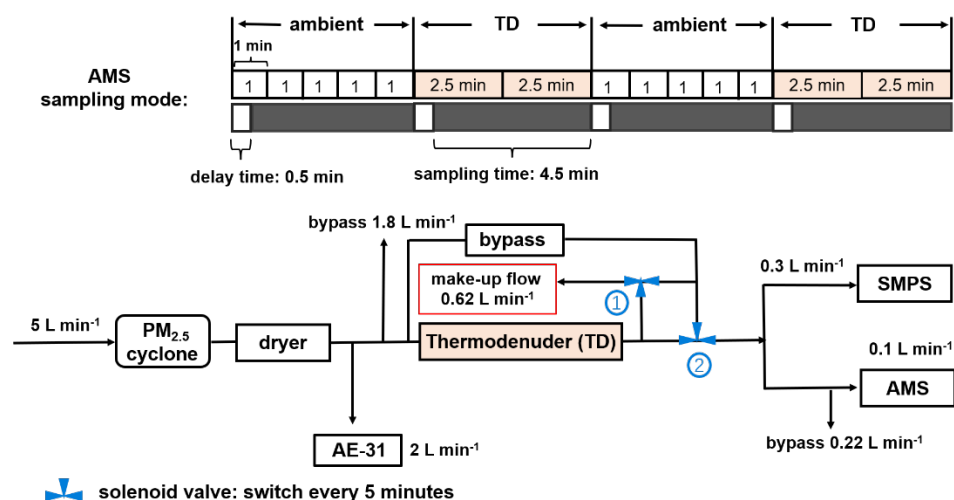


Figure S1. Brief schematic plot of sampling line in this campaign. The two solenoid valves control the switch of AMS and SMPS sampling lines to be ambient or TD lines. No matter whether ambient or TD lines were sampled by the SMPS and AMS, there is always a make-up flow to sample the other line for refreshing the air in the pipes.

R1.2: Lines 159-163: I would suggest describing a bit more details on why four factors were chosen, in particular, one aged-HOA factor was chosen instead of two HOA factors in this study.

A1.2: Thanks for the reviewer’s suggestion. A more detailed description of how to determine the OA factors, especially on aged-HOA is added in S1.1 in supporting information.

“At first, unconstrained source apportionment was conducted (seed=0) using PMF Evaluation Tool (PET, version 2.08) (Ulbrich et al., 2009). As the  $Q/Q_{exp}$  decreases (Fig. S3), no biomass burning factor was resolved in 3-4 factor solutions (Figs. S4 and S5). However, biomass burning was indeed seen during the campaign. Biomass burning-related factor was resolved when 5-7 factors were chosen, while they are not applicable due to splitting OOA factors (for example 5-

factor solution in Fig. S6). Thus, the ME-2 method was applied here. As mentioned in the PMF results, it can be found that 4-5 factors are better solutions, because fewer factors cannot resolve the BBOA factor, whereas more factors will result in meaningless OOA factors. Then, we constrained HOA (from Beijing) and BBOA (from Changdao) in ambient and ambient + TD datasets using SoFi v6.81 with different  $\alpha$  values from 0 to 1, where  $\alpha$  value represents the constrained extent in the standard mass spectral profile (Canonaco et al., 2013). To ensure the results of source apportionment, OA factors from ambient and ambient + TD datasets should show similar variations. However, time series from ambient and ambient + TD are different when 4 factors with  $\alpha$  value of 0 were chosen (Fig. S7), thus 4 factors with HOA and BBOA being constrained in ME-2 here is not the best solution. When 5 factors were chosen, a splitting of the HOA time series was found (Fig. S8). The constrained HOA shows very low contributions to total OA (< 4 %) and is noisy, especially during the TD sampling. Such noisy time series will lead to a large uncertainty when calculating MFR (mass fraction remaining). Meanwhile, the constrained HOA factor exhibits a very similar variation to the aged-HOA here (Fig. S9,  $R=0.52$ ). Thus, we do not think the 5-factor solution with both HOA and BBOA being constrained is good as well. Instead, we only constrain BBOA without HOA, since the aged-HOA can be resolved in PMF. Here, strong BBOA obtained from the Changdao campaign, which was conducted in a similar season and nearby location to Dongying (Hu et al., 2013), was chosen. A difference exists in the OOA2 factor between the time series of ambient and ambient + TD in the 5-factor solution (Fig. S10). Therefore, 4 factors with BBOA being constrained ( $\alpha$  value=0) is the most environmentally meaningful solution. As shown in Fig. S11, there is a good correlation between the ambient and ambient + TD datasets, which can be used to investigate the volatilities of different OA factors.’

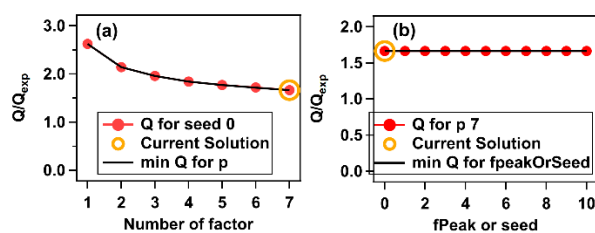


Figure S3. Values of (a)  $Q/Q_{exp}$  of different solutions and (b) fpeaks or seeds for free PMF.

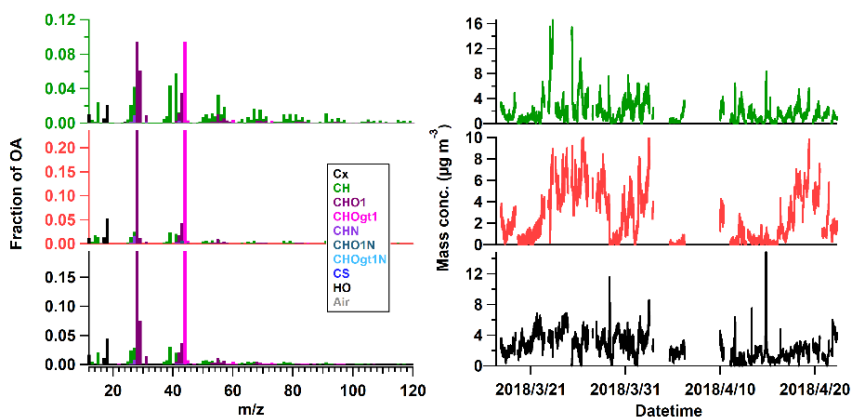


Figure S4. 3-factor solution of free PMF results.

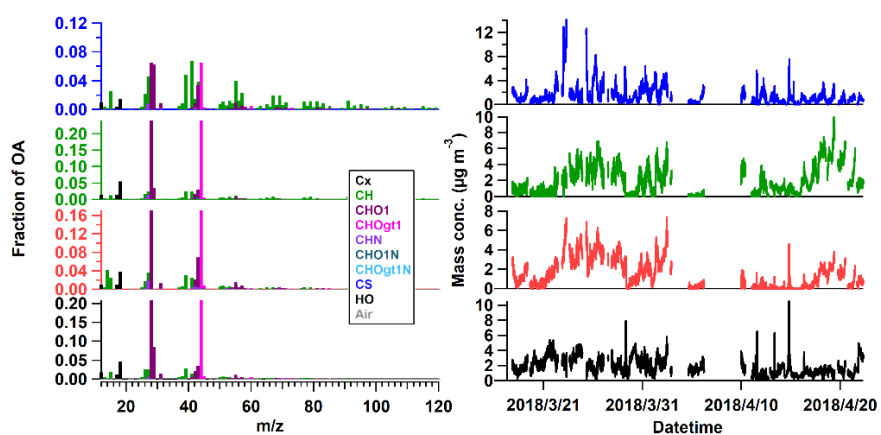


Figure S5. 4-factor solution of free PMF results.

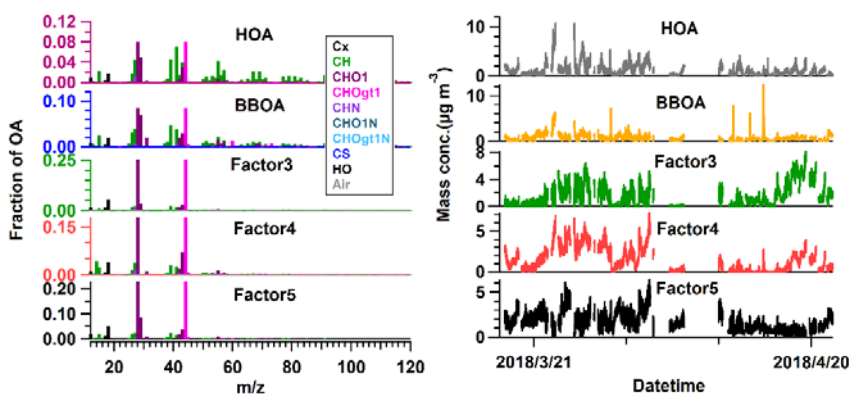


Figure S6. 5-factor solution of free PMF results. Splitting OOA factors were found for Factors 3-5.

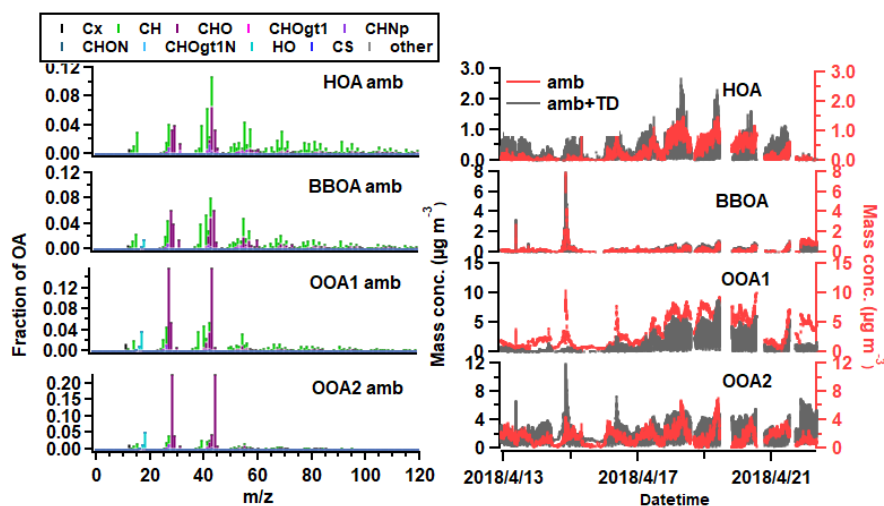


Figure S7. Comparison of OA factors variations between ambient (red) and ambient + TD (grey) resolved by ME-2 when constraining both HOA and BBOA factors. The solution of four factors were shown here.

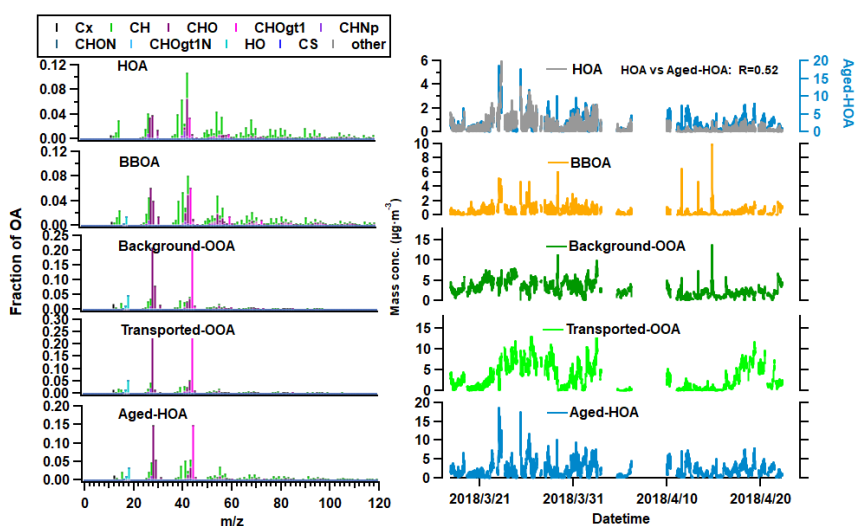


Figure S8. Spectra and time series of 5 factors when constraining both HOA and BBOA. The constrained-HOA show a good correlation with aged HOA.

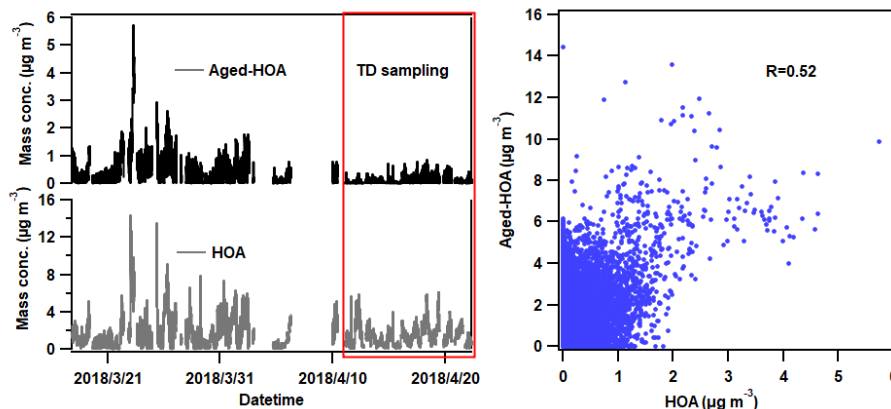


Figure S9. Comparison of time series between constrained HOA and aged-HOA of 5-factor solution when constraining both HOA and BBOA in ME-2.

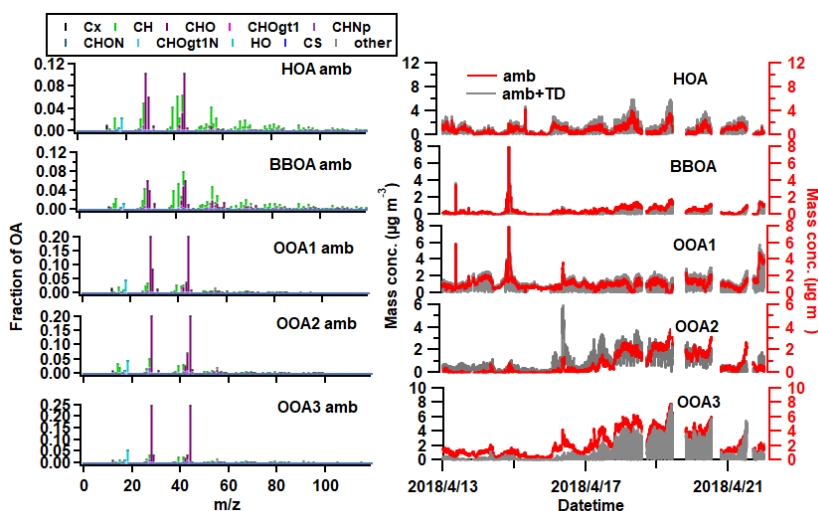


Figure S10. The 5-factor solution when only BBOA was constrained in ME-2.

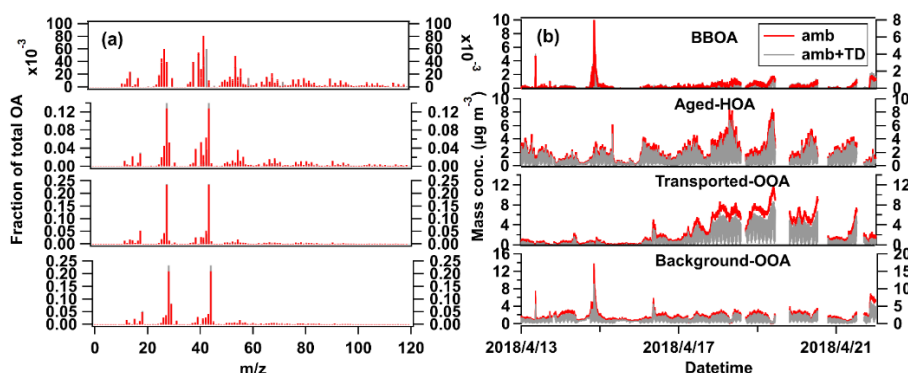


Figure S11. Comparison of OA factors and spectra between ambient (red) and ambient + TD (grey) resolved by ME-2 when only constraining BBOA.

R1.3: Line 173: The sampling flow was switched between TD and bypass every 4 min while the time resolution of SMPS measurement is 5 min. Will this lead to a mixed bypass and TD sample for each

measurement of SMPS? Please clarify.

**A1.3:** Sorry for causing confusion in the description of the sampling strategy. This is a typo. Actually, the temporal resolution between bypass and TD is 5 minutes, not 4 minutes. Thus, one point was measured by SMPS during each switch. The brief sampling mode is shown in the updated Fig. S1. In addition to the sampling by the instruments, a make-up flow was set to refresh the air in the TD and ambient (bypass) lines. E.g., when the TD line was sampled by the instruments, the air in the ambient line was also drawn by the make-up flow, vice versa. The make-up flow line was set at the same flow rate ( $0.62 \text{ L min}^{-1}$ ) by the air pump as the instruments sampling line. Therefore, the mixing of the bypass and TD points only occurred in the pipeline after switching valves, and the estimated mixing time is about 3-4s. To avoid this, we set a delay time (30s) on AMS and SMPS sampling during each switch to minimize the influences of mixing between ambient and TD sampling lines. The description was corrected in the main text.

**“The setup of the TD-AMS system in this study is shown in Fig. S1, where sampling flow was fast-switched to TD or bypass (ambient) paths at a time resolution of 5 minutes before being sampled by the AMS and SMPS. The switch of ambient and TD lines was controlled by the solenoid valve. When the instruments sample the ambient or TD lines, a make-up flow line with the same flow rate ( $0.62 \text{ L min}^{-1}$ ) was set to refresh the air in the other sampling line by the air pump. The residence time after solenoid valves is about 3-4s. To avoid the mixing of air between the ambient and TD lines, a delay time of 30s after each switch was set in the sampling strategy of AMS and SMPS instruments. In the TD line, the estimated residence time through the 55 cm heating section is 20.2 seconds, which is comparable with that (21.2 seconds) used by Huffman et al. (2008; 2009a; b).”**

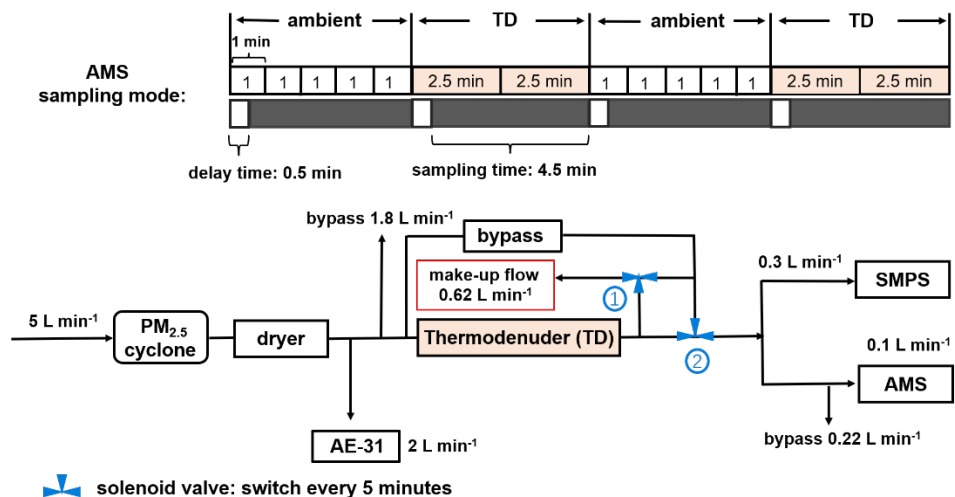


**Figure S1.** Brief schematic plot of sampling line in this campaign. The two solenoid valves control the switch of AMS and SMPS sampling lines to be ambient or TD lines. No matter whether ambient or TD lines were sampled by the SMPS and AMS, there is always a make-up flow to sample the other line for refreshing the air in the pipes.

**R1.4:** Lines 295-299: It is surprising that the O:C of aged-HOA can be that large during transport from surrounding urban areas. How long would it take for the vehicle emissions transport to this site? Is it possible that HOA undergoes aqueous oxidation and leads to a large increase of the O:C?

**A1.4:** It is hard to calculate the transportation time because the wind speed and emission location are uncertain. According to Fig. 5c2, the high concentrations of aged-HOA are probably from Dongying city (about 60 km away) and northern Jiangsu province (about 500 km away). We assume that the wind speed with long-distance transport should be above 7.2 km/h. In addition, the highest wind speed is about 16 km/h as shown in Fig. 5c1. Therefore, we estimate that it will take 4-8 hours to transport vehicle emissions from Dongying city. And if it is transported from Jiangsu, it will take 31-70 hours. HOA is thereby more aged than those of other studies. We clarified it in the main text:

“In addition, aged-HOA has the characterization of secondary sources. The average O:C value of aged-HOA in this campaign is 0.55, which is out of the range of O:C of HOA observed in China (0.05–0.44) (Hu et al., 2013; Zhou et al., 2020; Hu et al., 2016c). The high O:C value of aged-HOA in this study may be caused by long-distance transport from surrounding urban/town areas (Fig. 1a). Based on the bivariate polar plot and PCSF analysis in Fig. 5c, the higher aged-HOA

concentration is in accord with urban plumes originating from the west to south region, where Dongying city and northern Jiangsu are also on this path. It generally will take 4-8 hours for the vehicle emissions to be transported from Dongying and 31-70 hours from northern Jiangsu () to this site at a relatively high wind speed (7-16 km/h).”

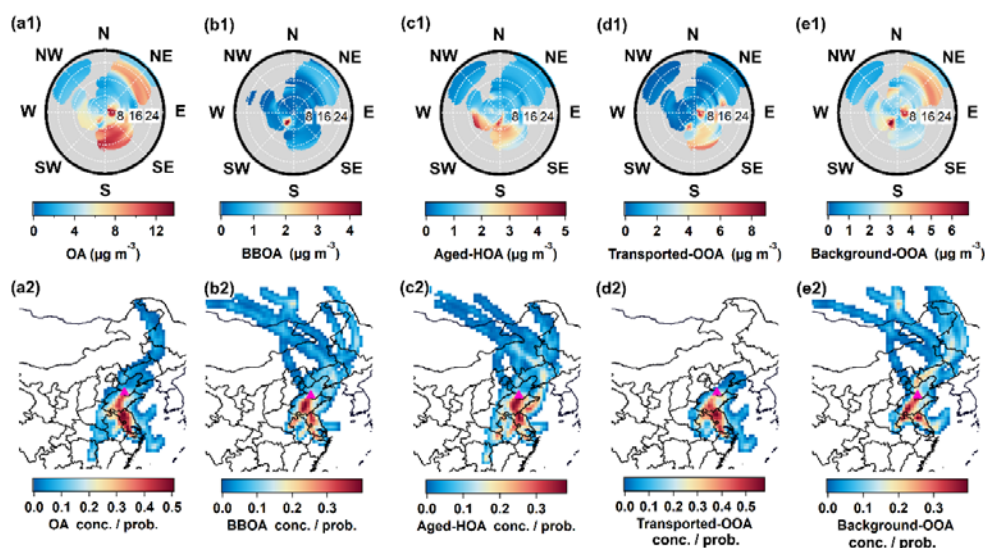


Figure 5. Bivariate polar plots and PSCF results of organic components, including (a1, a2) total OA; (b1, b2) BBOA; (c1, c2) aged-HOA; (d1, d2) transported-OOA; (e1, e2) background-OOA. The unit of wind speed is  $\text{km h}^{-1}$ .

Since the RH seldom goes above 80%, there is no clear evidence to support that the aqueous reaction can contribute to the aging of HOA in this study. In Fig. A1, the aged-HOA also does not show a clear variation as a function of RH. Thus, we prefer not to mention this to cause extra confusion.

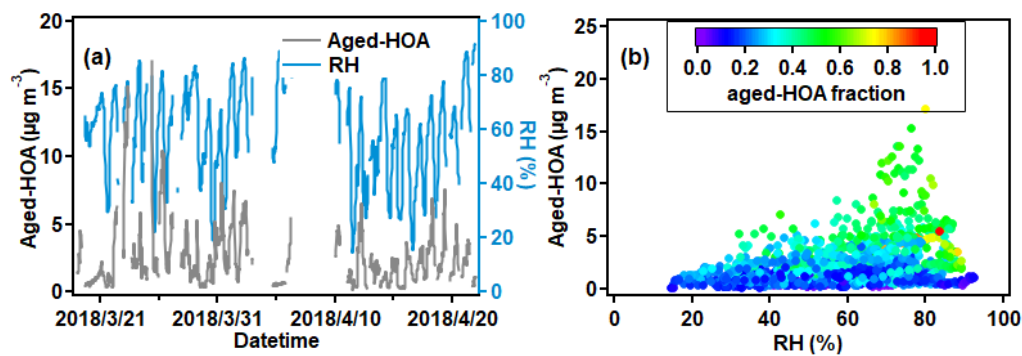


Figure A1. (a) Time series of mass concentration of aged-HOA and RH. (b) The scatter plots between aged-HOA and RH.

**R1.5:** Lines 438-440: Is there any other evidence that oligomers are formed? For example, is there a significant increase of the larger ions ( $m/z > 150$ ) in the AMS spectra?

**A1.5:** It is hard to detect oligomers using AMS without original molecular information. As suggested by the reviewer, we calculated the average fraction of OA ions (UMR, V-mode) during the campaign as a function of different TD temperatures. We found a slight enhancement of OA at higher ranges of  $m/z$  ( $>300$ ) when the temperature is above  $200\text{ }^{\circ}\text{C}$ , supporting the high residual might be partially contributed by the oligomers. To clarify this, we added Fig. S22 and modified the original sentences as:

**“Extremely low volatilities in the ambient air indicate that oligomers may exist in the aged plumes.”**

**“In addition, we investigated the OA spectrum as a function of TD temperature, as shown in Fig. S22. When the TD temperature is above  $200\text{ }^{\circ}\text{C}$ , the fraction signals of some ions at  $m/z >300$  were enhanced, implying the existence of oligomers.”**

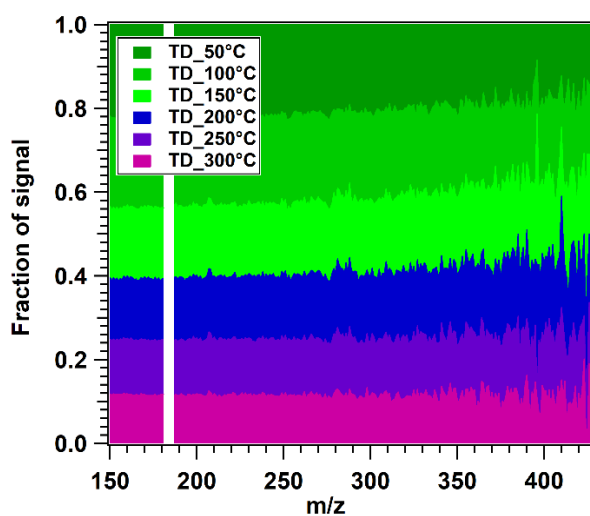


**Figure S22. The fraction of ions ( $m/z$  150-300) detected by AMS (unit mass resolution, V mode) at different TD temperatures. .**

**R1.6:** Lines 454-455: Can the authors provide more details on how the dilution is performed?

**A1.6:** We used the model rather than the experiment to evaluate the relative mass loss ( $E_{\text{loss}}$ ) under  $25^{\circ}\text{C}$  due to dilution. Based on the measured volatility, we can theoretically calculate the upper-limit sensitivity base on the following equation by assuming that the dilution air is clean. To clarify this, we revised the

original main text as:

“Further, we investigated the evaporation loss of OA due to dilution according to the theoretical equation (Cappa and Jimenez, 2010), which is mainly dependent upon its non-volatile/volatile fraction.

$$E_{\text{loss}}=100\% \left[ 1 - \frac{C_{\text{OA}}(\text{DF})}{C_{\text{OA}}(0)/\text{DF}} \right] \quad (2)$$

Where DF is the dilution factor, here we assume a 30 times dilution.  $C_{\text{OA}}(\text{DF})$  is the re-equilibrated  $C_{\text{OA}}$  after dilution,  $C_{\text{OA}}(0)$  is the OA mass before dilution, and  $E_{\text{loss}}$  is the relative mass loss due to evaporation of semivolatile components.”

### **Technical comments:**

**R1.7:** Line 205: The font of the website is inconsistent with the main text.

**A1.7:** Thanks for the reviewer’s reminder, we have revised the font of the website.

“(http://ready.arl.noaa.gov/HYSPLIT.php)”

### **Anonymous Referee #2**

#### **General comments:**

The manuscript by Tingting Feng et al. investigated the aging impact on sources, volatility, and viscosity of organic aerosols in Dongying. They found that the BBOA was the most volatile OA factor, followed by aged-HOA, transported-OOA and background-OOA. In addition, the estimated mixing time of OA varied dramatically from minutes at night to years in the afternoon, emphasizing the necessity to consider its dynamic kinetic limits when modeling OA. The topic fits well within the scope of Atmospheric Chemistry and Physics. This manuscript is generally well written. Before its publication, the following comments need to be addressed.

#### **Specific Comments:**

**R2.1:** More information needs to be provided to support source apportionment results in the background-OOA and transported-OOA. For example, the background-OOA did show a relative flat diurnal variation. However, the elevated loading of background-OOA was occurred after excluding the impacts of PBL. In addition, the lower O/C of transported-OOA compared to background-OOA was observed. Is such difference in the oxidation state one of the reasons that you name background-OOA and transported-OOA? If so, please list the references and explain the reasons. In addition, is there any other evidences to support that factor 2 is related to the ageing of HOA (rather than COA, CCOA or other primary emissions)? What about the correlations of aged-HOA profiles in this study with the aged traffic emissions in laboratory studies?

**A2.1:** There exist two OOA factors with high oxidation states in the ME-2 results. We define the two factors based on the characterization of their sources. First, compared with background-OOA, the mass concentration of transported-OOA varies more sharply, which is significantly influenced by the transported pollutants at high-speed winds. Combined with the PSCF and bivariate polar plots, transported-OOA is correlated with secondary inorganic species (nitrate and sulfate), which are most transported from urban cities when the south winds dominated, thus named transported-OOA. As for the background-OOA, it was influenced by plumes from all directions, which represents the characterization of background aerosols in NCP. And we did not find any secondary species that can correlate well with this factor except m/z 44. In addition, the background-OOA shows much lower volatilities than the transported OOA, suggesting the background OOA is very aged. For the diurnal variation, the observation site is a background site, which is more influenced by the transportation from upwind regions. Thus, the diurnal variation of different species is determined by the plumes from heavily polluted regions and the variation of diurnal profiles is not as representative as those in the urban cities. Therefore, we deleted the description of “flat diurnal variation” in the main text. Combing all the evidence, we named this factor as background-OOA. We have revised the original main text as:

**“The transported-OOA shows good correlations with secondary inorganic sulfate and nitrate ( $R = 0.81$  and  $0.83$  shown in Fig. S14, respectively), consistent with its secondary origins of OOA (He et al., 2011; Huang et al., 2020; Zhang et al., 2005). The regression ratio between transported-OOA vs. sulfate + nitrate is around  $0.84$ , within the range obtained in NCP areas ( $0.51$ – $0.93$ ) (Sun et al., 2016; Sun et al., 2012; Huang et al., 2010). Similar to secondary inorganic species, the higher mass**

concentration of transported-OOA is also driven by the south winds, thus named transported-OOA. The bivariate polar plots and PSCF results (Fig. 5d) show that the higher transported-OOA concentration might correspond to the transport processes from urban emissions located in the southern region of the sampling site. On the contrary, the background-OOA shows enhanced mass concentrations in all directions (Fig. 5e1) compared with transported-OOA, indicating its background origins, and representing the background concentration in NCP ( $2.6 \pm 1.6 \mu\text{g m}^{-3}$ ). In addition, in section 3.4.2, we found very low volatility of background-OOA, confirming it is very aged in the ambient air. ”

In this study, aged-HOA was identified by the characteristics of the spectrum and mass concentration variation. As suggested by the reviewer, we added more evidence to show why the aged HOA is not COA, CCOA, or other primary emissions but is more related to vehicle emissions.

“In this solution, the BBOA factor was resolved by constraining the BBOA spectrum from the Changdao campaign. The other POA is considered to be aged-HOA rather than COA/CCOA for the following reasons: (1) First of all, we do not identify the PAH ions with high abundance in this mass spectrum like CCOA in the spring of Changdao (Fig. S12(c)), so CCOA is not the priority we considered here. (2) The ratio between  $f_{55}$  versus  $f_{57}$  is different in HOA (0.9-1.1) and COA (2.2-2.8) spectra, which is driven by the oxygen-containing ions,  $\text{C}_3\text{H}_3\text{O}^+$  and  $\text{C}_3\text{H}_5\text{O}^+$  (Mohr et al., 2012). In this study, the scatterplots of  $f_{55}$  versus  $f_{57}$ , which subtracted the interferences of OOA, are closer to the COA source in the urban areas than HOA sources (Fig. S12(d)). However, the higher  $f_{55}/f_{57}$  value in ambient OA is not driven by the aged-HOA. E.g., as the fraction of aged-HOA in total OA goes up, the  $f_{55}$  vs  $f_{57}$  ratios do not change (Fig. S12(d)). The value of  $f_{55}$  versus  $f_{57}$  of aged-HOA is 1.8, which is also similar to that of BBOA and lower than those of the other two OOA factors (Fig. S12(d)). Thus, the higher value of  $f_{55}$  vs  $f_{57}$  here is probably due to the oxidation of HOA during transportation. To further investigate if the cooking impact the OA in this study, another cooking tracer  $f_{98}$  was investigated here. We compared the scatterplots between  $f_{44}$  vs.  $f_{98}$  with other field campaigns that were impacted by the cooking or not. As shown in Fig. S13. no enhancement of  $f_{98}$  was found in this study compared to other studies, suggesting the cooking did not show an obvious impact on OA observed in this site. In addition, the two peaks in the dining time were not found in

the aged-HOA factor. The evidence to support the aged-HOA is from vehicle emissions based on the relationship between some traffic tracers and aged-HOA. As mentioned in Fig. S14, factor 2 (that is aged-HOA) is highly correlated with typical traffic tracers, such as BC, NO<sub>2</sub>, and benzene (R>0.6). Therefore, the other POA factor is considered as HOA originated from vehicle emissions in this study. In addition, when the standard HOA spectrum was constrained, the time series of that POA is similar to the trend of aged-HOA (Fig. S15), which confirmed the existence of aged-HOA factor.”

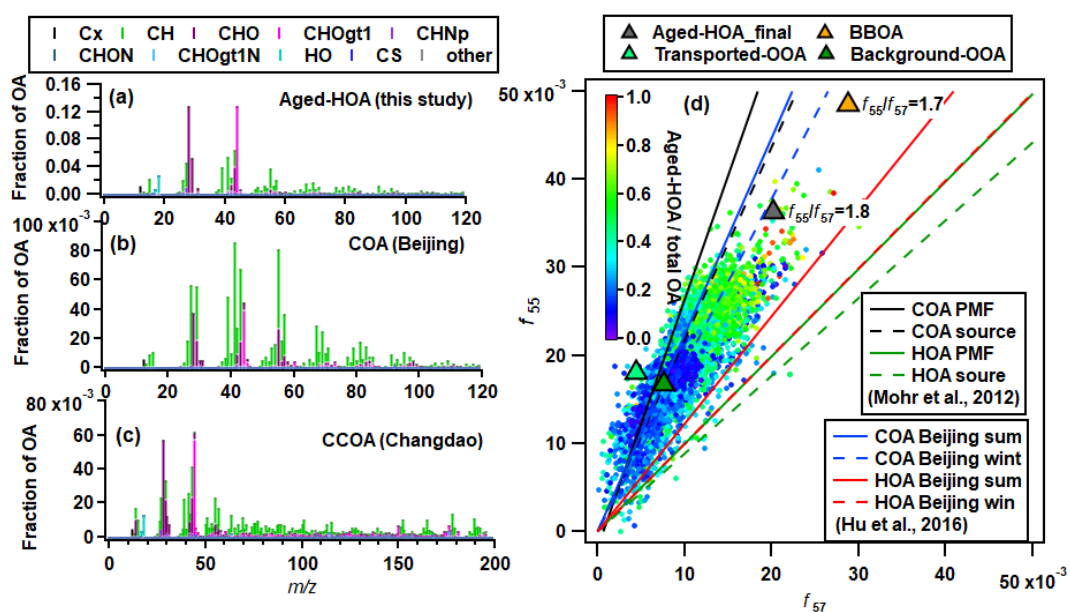


Figure S12. Spectra of (a) aged-HOA in this study; (b) COA in Beijing; (c) CCOA in Changdao; (d) Scatterplots between  $f_{55}$  versus  $f_{57}$  in this study. The lines in panel (d) are the range of different sources reported by Mohr et al. (2012) and Hu et al. (2016).

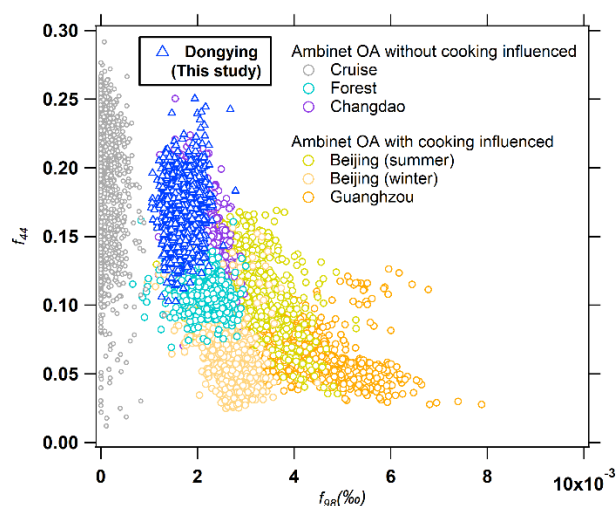


Figure S13. Scatterplots of  $f_{44}$  vs.  $f_{98}$  from different studies, including observation sites with/without cooking influenced.

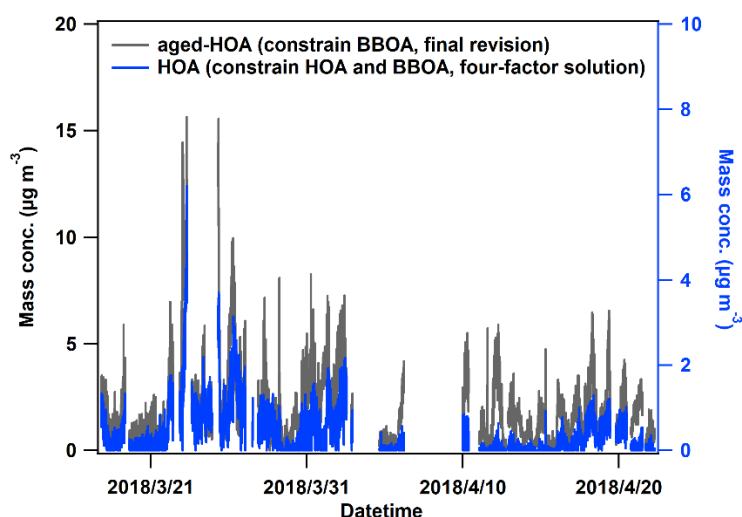


Figure S15. Time series of aged-HOA and POA that resolved when constrained standard HOA spectrum.”

Similar to spectra from the previous study (Zhu et al., 2021), the oxygenated ions in aged-HOA factor were also observed in this study because of the oxidation of fresh HOA, as shown in the following Fig. A2. However, the spectrum of aged-HOA in this study was substantially contributed from alkyl fragments, which may be influenced by the mixing of fresh HOA, while the aged HOA generated in the laboratory oxidation study generally showed less contribution from alkyl fragments, especially at  $m/z > 44$ . Thus, the aged-HOA in the ambient air of this study is different from oxidized HOA in the laboratory

experiments. We cannot find the raw data of the aged HOA from Zhu et al. (2021). Thus, the scatter plots between these factors and aged factors as suggested by the review cannot be plotted here.

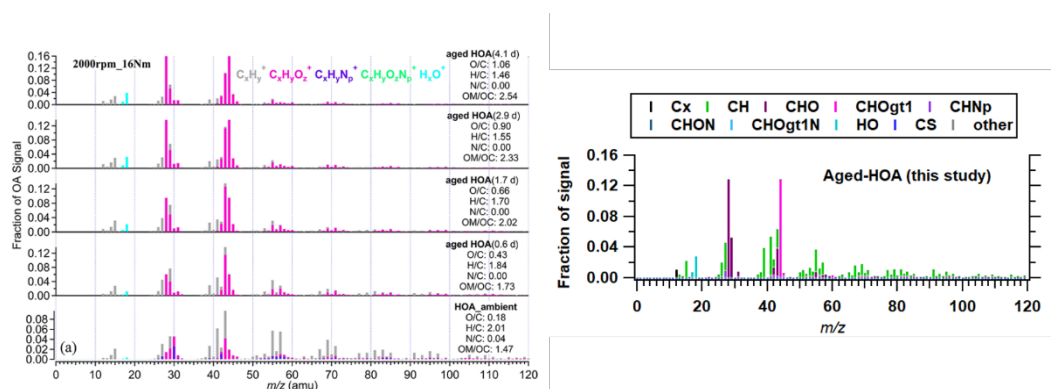


Figure A2. Spectra of aged-HOA from Zhu et al. (2021) (left) and this study (right)

**R2.2:** Are there any specific reasons for using a constant CE (0.5), rather than CDCE? How about the neutralization in ambient air and each TD temperature? Please mention it here.

**A2.2:** There might be a misunderstanding. We applied the CDCE rather than a constant CE to correct the particle bounce loss in AMS. The time series of CDCE can be found in the following Fig. A3. The average value of CDCE is around  $0.52 \pm 0.04$ . To clarify this, we add the abbreviation of “CDCE” in the main text and revised the sentences.

“Taking into account particle loss in AMS, the chemical composition-dependent CE (CDCE) followed by Middlebrook et al. (2012) was applied to correct mass concentration. The average value of CDCE is  $0.52 \pm 0.04$ .”

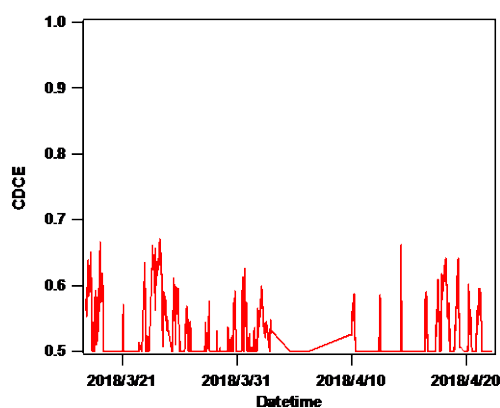


Figure A3. Time series of estimated CDCE in this study.

The NH<sub>4</sub> balance accounting for organic nitrate in the total nitrate signal is shown in Fig. A4. The aerosols are almost neutral in the ambient air whether the organic nitrate in total nitrate signal was considered or not. Thus, the average value of CDCE = 0.52 is reasonable. The ammonium balance as a function of TD temperature was already shown in Fig. 6f in the original main text.

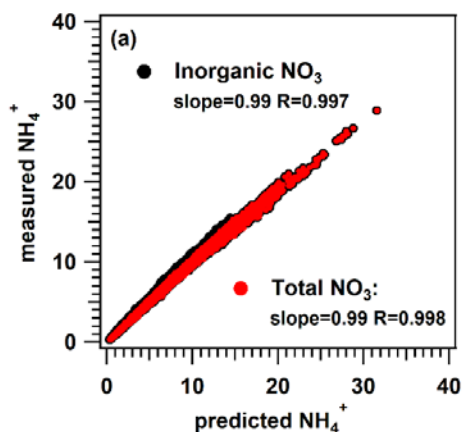


Figure A4. NH<sub>4</sub> balance calculated by total nitrate and inorganic nitrate.

**R2.3:** How did you measure the organic nitrate? Did you exclude the impacts of organic nitrates on the measured/predicted NH<sub>4</sub> in Fig. 6(f). I am also curious the lower mass concentrations of organic nitrate in the polluted periods compared to entire periods. Please elaborate.

**A2.3:** The impacts of organic nitrates on the measured/predicted NH<sub>4</sub> can be found in A2.2, which shows negligible influences. We estimated the fraction of particle organic nitrate ( $f_{\text{RONO}_2}$ ) in this study using the NO<sub>2</sub><sup>+</sup>/NO<sup>+</sup> ratio method proposed by Farmer et al. (2010) and Day et al. (2022). The detailed information can be found in Section 1.4 of the supporting information,

**“During the calibration, the measured NO<sub>x</sub> ratio (NO<sub>2</sub><sup>+</sup>/NO<sup>+</sup>) of standard ammonium nitrate particles ( $R_{\text{NH}_4\text{NO}_3}$ ) was determined to be 0.28 (Fig. S16a). The NO<sub>2</sub><sup>+</sup>/NO<sup>+</sup> ratio of organic nitrate ( $R_{\text{ONO}_2}$ ) was estimated by dividing  $R_{\text{NH}_4\text{NO}_3}$  by a factor of 2.75 proposed by Day et al. (2022), thus the  $R_{\text{ONO}_2}$  ratio in this study is 0.1. The fraction of organic nitrate and inorganic nitrate can be estimated based on the following equations (Farmer et al., 2010):**

$$f_{\text{RONO}_2} = \frac{(R_{\text{amb}} - R_{\text{NH}_4\text{NO}_3})(1 + R_{\text{ONO}_2})}{(R_{\text{ONO}_2} - R_{\text{NH}_4\text{NO}_3})(1 + R_{\text{amb}})} \quad (12)$$

$$f_{\text{RONO}_2} = 1 \quad (f_{\text{RONO}_2} > 1) \quad (13)$$

$$f_{\text{NH}_4\text{NO}_3} = 1 - f_{\text{RONO}_2} \quad (0 < f_{\text{RONO}_2} < 1) \quad (14)$$

$$f_{\text{NH}_4\text{NO}_3} = 1 \quad (f_{\text{RONO}_2} < 0) \quad (15)''$$

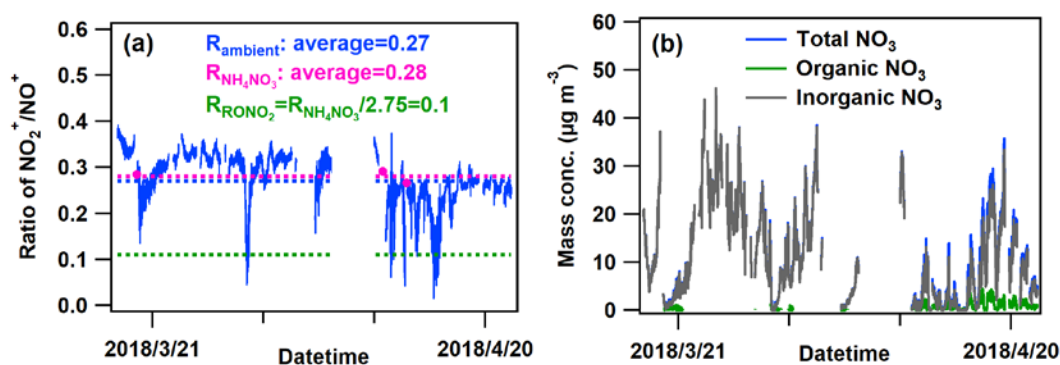


Figure S16. (a) Time series of the ratio of NO<sub>2</sub><sup>+</sup>/NO<sup>+</sup> for ambient nitrate (R<sub>ambient</sub>), pure ammonium nitrate (R<sub>NH<sub>4</sub>NO<sub>3</sub></sub>) and organic nitrate particles (R<sub>RONO<sub>2</sub></sub>); (b) Time series of organic and inorganic nitrate based on the ratios of NO<sub>2</sub><sup>+</sup>/NO<sup>+</sup> (Farmer et al., 2010; Day et al., 2021).

During the polluted period, the enhanced nitrate signal was mainly contributed by the inorganic nitrate. E.g., Day et al. (2022) found the fraction of organic nitrate in total nitrate decreases as a function of total nitrate by summarizing different field campaigns. As shown in Fig. A5. Thus, it is reasonable that organic nitrate concentration is low and its fraction in total aerosol is also lower during the polluted periods in urban areas.

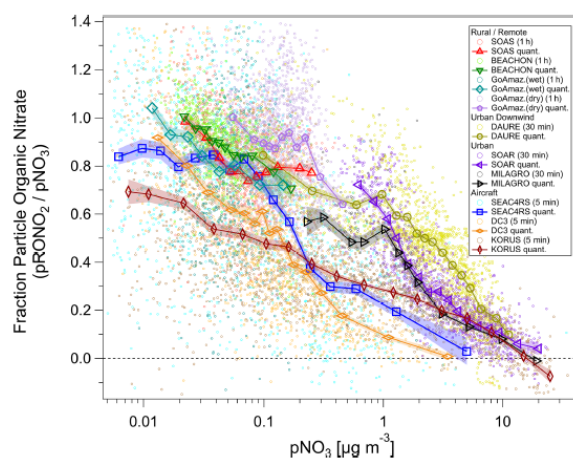


Figure A5. Fraction of total non-refractory submicron nitrate that is organic ( $f_{\text{pRONO}_2}$ ) vs. total nitrate concentration (pNO<sub>3</sub>) for several ground and aircraft campaigns (Day et al., 2022).

**R2.4:** The discussion regarding oligomers should be backed by the evidence rather than speculated upon at all throughout the manuscript.

**A2.4:** We show the spectrum of OA as a function of TD to support this deduction. The more detailed information refers to A1.5.

**R2.5:** Did you assess how long it takes to reach stability after switching? In my viewpoint, there might be a significant uncertainty using the switched time of 4 min. The authors need to address such uncertainties in the revised manuscript.

**A2.5:** We have updated the sampling mode in Fig. S1. The sampling cycle is 5 min in order to reduce the uncertainty. The more detailed information has been clarified in A1.3.

**R2.6:** Are there any other metal containing constituents' measurements to support your assumptions (e.g., line 365-367)? Looking into the HR data(e.g., Na<sup>+</sup>, K<sup>+</sup> and Pb<sup>+</sup>) would be helpful.

**A2.6:** We have checked the HR data for these metal ions. However, the time series of Na<sup>+</sup> and K<sup>+</sup> did not show meaningful variation as shown in Fig. A6. The Pb<sup>2+</sup> ion cannot be fitted in the AMS spectrum. Furthermore, we looked into the correlation between all the metal cations (K, Pb, Ga, Ru, Rb, Se, Zn, Cd) and Cl<sup>-</sup> based on the offline measurement with filter sampling. The highest correlation coefficient was found between K and Cl (R=0.54), and Pb and Cl (0.51), others are below 0.4. The positive correlation between K<sup>+</sup> and Cl<sup>-</sup>, as well as Pb<sup>2+</sup> and Cl<sup>-</sup>, indicates the possible existence of PbCl<sub>2</sub> and KCl in the ambient aerosols. To clarify this, a supporting information figure and corresponding sentences in the main text were added:

**“The positive correlations between Cl<sup>-</sup> vs. Pb<sup>2+</sup> (R=0.51), as well as Cl<sup>-</sup> vs. K<sup>+</sup> (R=0.54) supports this probability (Fig. S21).”**

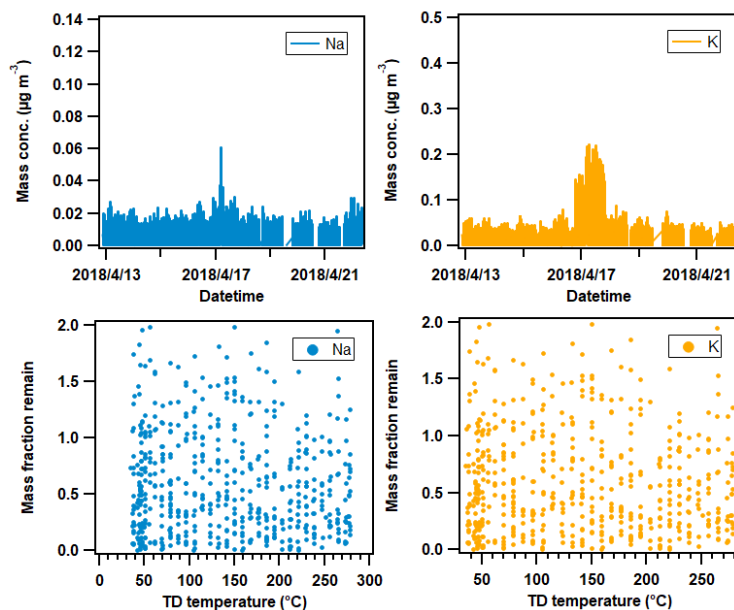


Figure A6. Time series and mass fraction remaining of  $\text{Na}^+$  and  $\text{K}^+$  measured by AMS.

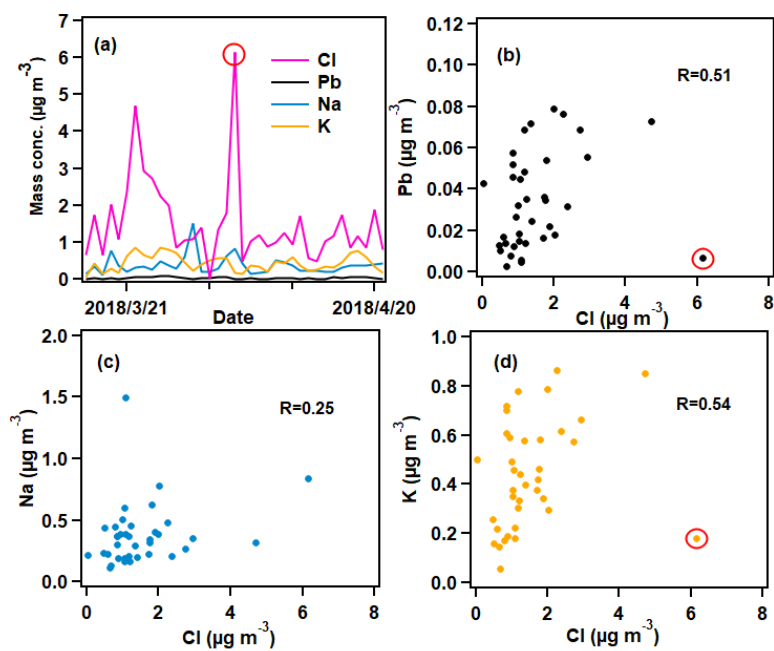


Figure S21. Time series  $\text{Na}^+$ ,  $\text{K}^+$ ,  $\text{Pb}^{2+}$ , and  $\text{Cl}^-$  of measured by offline line technique, as well as the scatterplots between anions and cations. The discrete points surrounded by red circles are not used when calculating Pearson correlation coefficients.

**R2.7:** The author has not discussed the inlet used for dilution fully. An experimental design for dilution needs to be included in Section 2. In addition, a discussion about the additional mass losses of four OA

factors as functions of the dilution factor is irrelevant for the section 3.4.2.

**A2.7:** Sorry for the confusion. The dilution curve here is not measured but theoretically estimated based on the OA volatility distribution. The detailed estimation process is added in the main text, which can be referred to A1.6. Fig. 8f shows the mass losses of four-OA factors after dilution to simulate the evaporated mass fraction of OA after being transported to the downwind areas, which is determined directly based on the OA volatility distribution. Thus, this part is closely related to section 3.4.2, which mainly focuses on the volatility distribution of OA and OA factors.

8 Line 116: Inaccurate "PM<sub>1</sub>". Do you mean "NR-PM<sub>1</sub>"?

**A2.8:** Yes, corrected.

## References

- Canonaco, F., Crippa, M., Slowik, J. G., Baltensperger, U., and Prévôt, A. S. H.: SoFi, an IGOR-based interface for the efficient use of the generalized multilinear engine (ME-2) for the source apportionment: ME-2 application to aerosol mass spectrometer data, *Atmospheric Measurement Techniques*, 6, 3649-3661, 10.5194/amt-6-3649-2013, 2013.
- Cappa, C. D. and Jimenez, J. L.: Quantitative estimates of the volatility of ambient organic aerosol, *Atmospheric Chemistry and Physics*, 10, 5409-5424, 10.5194/acp-10-5409-2010, 2010.
- Day, D. A., Campuzano-Jost, P., Nault, B. A., Palm, B. B., Hu, W., Guo, H., Wooldridge, P. J., Cohen, R. C., Docherty, K. S., Huffman, J. A., de Sá, S. S., Martin, S. T., and Jimenez, J. L.: A Systematic Re-evaluation of Methods for Quantification of Bulk Particle-phase Organic Nitrates Using Real-time Aerosol Mass Spectrometry, *Atmos. Meas. Tech. Discuss.*, 2021, 1-35, 10.5194/amt-2021-263, 2021.
- Day, D. A., Campuzano-Jost, P., Nault, B. A., Palm, B. B., Hu, W., Guo, H., Wooldridge, P. J., Cohen, R. C., Docherty, K. S., Huffman, J. A., de Sá, S. S., Martin, S. T., and Jimenez, J. L.: A systematic re-evaluation of methods for quantification of bulk particle-phase organic nitrates using real-time aerosol mass spectrometry, *Atmospheric Measurement Techniques*, 15, 459-483, 10.5194/amt-15-459-2022, 2022.
- Farmer, D. K., Matsunaga, A., Docherty, K. S., Surratt, J. D., Seinfeld, J. H., Ziemann, P. J., and Jimenez, J. L.: Response of an aerosol mass spectrometer to organonitrates and organosulfates and implications for atmospheric chemistry, *Proc Natl Acad Sci U S A*, 107, 6670-6675, 10.1073/pnas.0912340107, 2010.
- He, L.-Y., Huang, X.-F., Xue, L., Hu, M., Lin, Y., Zheng, J., Zhang, R., and Zhang, Y.-H.: Submicron aerosol analysis and organic source apportionment in an urban atmosphere in Pearl River Delta of China using high-resolution aerosol mass spectrometry, *Journal of Geophysical Research*, 116, 10.1029/2010jd014566, 2011.
- Hu, W., Hu, M., Hu, W., Jimenez, J. L., Yuan, B., Chen, W., Wang, M., Wu, Y., Chen, C., Wang, Z., Peng, J., Zeng, L., and Shao, M.: Chemical composition, sources, and aging process of submicron aerosols in Beijing: Contrast between summer and winter, *Journal of Geophysical Research: Atmospheres*, 121, 1955-1977, 10.1002/2015jd024020, 2016.

Hu, W. W., Hu, M., Yuan, B., Jimenez, J. L., Tang, Q., Peng, J. F., Hu, W., Shao, M., Wang, M., Zeng, L. M., Wu, Y. S., Gong, Z. H., Huang, X. F., and He, L. Y.: Insights on organic aerosol aging and the influence of coal combustion at a regional receptor site of central eastern China, *Atmospheric Chemistry and Physics*, 13, 10095-10112, 10.5194/acp-13-10095-2013, 2013.

Huang, R.-J., He, Y., Duan, J., Li, Y., Chen, Q., Zheng, Y., Chen, Y., Hu, W., Lin, C., Ni, H., Dai, W., Cao, J., Wu, Y., Zhang, R., Xu, W., Ovadnevaite, J., Ceburnis, D., Hoffmann, T., and O'Dowd, C. D.: Contrasting sources and processes of particulate species in haze days with low and high relative humidity in wintertime Beijing, *Atmospheric Chemistry and Physics*, 20, 9101-9114, 10.5194/acp-20-9101-2020, 2020.

Huang, X. F., He, L. Y., Hu, M., Canagaratna, M. R., Sun, Y., Zhang, Q., Zhu, T., Xue, L., Zeng, L. W., Liu, X. G., Zhang, Y. H., Jayne, J. T., Ng, N. L., and Worsnop, D. R.: Highly time-resolved chemical characterization of atmospheric submicron particles during 2008 Beijing Olympic Games using an Aerodyne High-Resolution Aerosol Mass Spectrometer, *Atmospheric Chemistry and Physics*, 10, 8933-8945, 10.5194/acp-10-8933-2010, 2010.

Huffman, J., Docherty, K., Aiken, A., Cubison, M., Ulbrich, I., DeCarlo, P., Sueper, D., Jayne, J., Worsnop, D., Ziemann, P., and Jimenez, J.: Chemically-resolved aerosol volatility measurements from two megacity field studies, *Atmospheric Chemistry and Physics*, 9, 10.5194/acpd-9-2645-2009, 2009a.

Huffman, J. A., Ziemann, P. J., Jayne, J. T., Worsnop, D. R., and Jimenez, J. L.: Development and Characterization of a Fast-Stepping/Scanning Thermodenuder for Chemically-Resolved Aerosol Volatility Measurements, *Aerosol Science and Technology*, 42, 395-407, 10.1080/02786820802104981, 2008.

Huffman, J. A., Docherty, K. S., Mohr, C., Cubison, M. J., Ulbrich, I. M., Ziemann, P. J., Onasch, T. B., and Jimenez, J. L.: Chemically-Resolved Volatility Measurements of Organic Aerosol from Different Sources, *Environmental Science & Technology*, 43, 5351-5357, 10.1021/es803539d, 2009b.

Middlebrook, A. M., Bahreini, R., Jimenez, J. L., and Canagaratna, M. R.: Evaluation of Composition-Dependent Collection Efficiencies for the Aerodyne Aerosol Mass Spectrometer using Field Data, *Aerosol Science and Technology*, 46, 258-271, 10.1080/02786826.2011.620041, 2012.

Mohr, C., DeCarlo, P. F., Heringa, M. F., Chirico, R., Slowik, J. G., Richter, R., Reche, C., Alastuey, A., Querol, X., Seco, R., Peñuelas, J., Jiménez, J. L., Crippa, M., Zimmermann, R., Baltensperger, U., and Prévôt, A. S. H.: Identification and quantification of organic aerosol from cooking and other sources in Barcelona using aerosol mass spectrometer data, *Atmospheric Chemistry and Physics*, 12, 1649-1665, 10.5194/acp-12-1649-2012, 2012.

Sun, Y., Wang, Z., Dong, H., Yang, T., Li, J., Pan, X., Chen, P., and Jayne, J. T.: Characterization of summer organic and inorganic aerosols in Beijing, China with an Aerosol Chemical Speciation Monitor, *Atmospheric Environment*, 51, 250-259, 10.1016/j.atmosenv.2012.01.013, 2012.

Sun, Y., Chen, C., Zhang, Y., Xu, W., Zhou, L., Cheng, X., Zheng, H., Ji, D., Li, J., Tang, X., Fu, P., and Wang, Z.: Rapid formation and evolution of an extreme haze episode in Northern China during winter 2015, *Sci Rep*, 6, 27151, 10.1038/srep27151, 2016.

Ulbrich, I. M., Canagaratna, M. R., Zhang, Q., Worsnop, D. R., and Jimenez, J. L.: Interpretation of organic components from Positive Matrix Factorization of aerosol mass spectrometric data, *Atmos. Chem. Phys.*, 9, 2891-2918, 10.5194/acp-9-2891-2009, 2009.

Zhang, Q., Worsnop, D. R., Canagaratna, M. R., and Jimenez, J. L.: Hydrocarbon-like and oxygenated organic aerosols in Pittsburgh: insights into sources and processes of organic aerosols, *Atmos. Chem. Phys.*, 5, 3289-3311, 10.5194/acp-5-3289-2005, 2005.

Zhu, W., Guo, S., Zhang, Z., Wang, H., Yu, Y., Chen, Z., Shen, R., Tan, R., Song, K., Liu, K., Tang, R., Liu, Y., Lou, S., Li, Y., Zhang, W., Zhang, Z., Shuai, S., Xu, H., Li, S., Chen, Y., Hu, M., Canonaco, F., and Prévôt, A. S. H.: Mass spectral characterization of secondary organic aerosol from urban cooking and vehicular sources, *Atmospheric Chemistry and Physics*, 21, 15065-15079, 10.5194/acp-21-15065-2021, 2021.